Cell Reports
Article

Dendritic Glutamate Receptor mRNAs Show Contingent Local Hotspot-Dependent Translational Dynamics

Tae Kyung Kim,[1] Jai-Yoon Sul,[1] Henrik Helmfors,[4] Ulo Langel,[4] Junhyong Kim,[2,3] and James Eberwine[1,3,*]
[1]Department of Pharmacology, Perelman School of Medicine, Philadelphia, PA 19104-6084, USA
[2]Department of Biology, School of Arts and Sciences, University of Pennsylvania, Philadelphia, PA 19104-6313, USA
[3]Penn Genome Frontiers Institute, University of Pennsylvania, John Morgan Building, Room 37, 36th and Hamilton Walk, Philadelphia, PA, 19104, USA
[4]Department of Neurochemistry, Stockholm University, S. Arrheniusv. 21A, SE-106 91 Stockholm, Sweden
*Correspondence: eberwine@upenn.edu
http://dx.doi.org/10.1016/j.celrep.2013.08.029

SUMMARY

Protein synthesis in neuronal dendrites underlies long-term memory formation in the brain. Local translation of reporter mRNAs has demonstrated translation in dendrites at focal points called translational hotspots. Various reports have shown that hundreds to thousands of mRNAs are localized to dendrites, yet the dynamics of translation of multiple dendritic mRNAs has remained elusive. Here, we show that the protein translational activities of two dendritically localized mRNAs are spatiotemporally complex but constrained by the translational hotspots in which they are colocalized. Cotransfection of glutamate receptor 2 (GluR2) and GluR4 mRNAs (engineered to encode different fluorescent proteins) into rat hippocampal neurons demonstrates a heterogeneous distribution of translational hotspots for the two mRNAs along dendrites. Stimulation with *s*-3,5-dihydroxy-phenylglycine modifies the translational dynamics of both of these RNAs in a complex saturable manner. These results suggest that the translational hotspot is a primary structural regulator of the simultaneous yet differential translation of multiple mRNAs in the neuronal dendrite.

INTRODUCTION

Local protein synthesis gives cells the ability to respond rapidly and selectively to extracellular stimuli. This is especially important in neurons that have highly polarized cell morphology and extended processes in which rapid structural and functional changes occur concurrently. Such structural and functional changes (i.e., synaptic plasticity) require new synthesis of proteins in the dendrite (Alberini, 1999; Goelet et al., 1986; Kang and Schuman, 1996; Sutton and Schuman, 2005). Consequently, the structural modification of synaptic junctions forms a mechanistic basis for a cellular model of learning and memory (Costa-Mattioli et al., 2009; Crino and Eberwine, 1996; Job and Eberwine, 2001; Sutton and Schuman, 2005). Local dendritic translation is known to be involved in memory-forming responses; however, the role of the local environment in regulating the translation of multiple dendritic mRNAs has been unexplored (Kang and Schuman, 1996; Crino and Eberwine, 1996).

Ionotropic α-amino-3-hydroxy-5-methyl-4-isoxazolepropionic acid receptors (AMPARs) are tetrameric receptors composed of a combination of four subunits, glutamate receptor 1 (GluR1)–GluR4, which are encoded by the genes *gria1–gria4*, respectively (Riedel et al., 2003). AMPARs mediate postsynaptic responses to glutamate differently depending on the combination of subunits present, which is dictated in part by patterns of mRNA expression and distribution, as well as by splicing variants and post-translational modifications (Greger and Esteban, 2007). Extracellular stimulation is known to trigger dendritic protein synthesis and the immediate restructuring of AMPARs that are part of long-term depression (LTD) in rat hippocampal neurons (Carroll et al., 1999; Ju et al., 2004; Kacharmina et al., 2000; Miyashiro et al., 1994). Hence, the rapid production of appropriate amounts of various subunits is critical for a cell's ability to respond rapidly to stimuli, but this process may be complicated by the limited amount of translational machinery in dendrites (Huber et al., 2000; Mameli et al., 2007; Schmid et al., 2008; Sutton et al., 2004). It is well known that hundreds of mRNAs are present in the dendrite and that an appropriate stimulus may trigger the initiation of their translation (Buckley et al., 2011; Dynes and Steward, 2007; Eberwine et al., 2002; Falley et al., 2009; Kacharmina et al., 2000; Rook et al., 2000). Previous studies in our lab have shown that GluR2 and GluR4 mRNAs are present at similar levels within the dendrite (Miyashiro et al., 1994), GluR2 is synthesized and inserted into the membrane in the dendrite (Kacharmina et al., 2000), GFP mRNA translation in a confined area (termed a "translational hotspot") can be measured using isolated dendrites from rat hippocampal neurons, and translational hotspots are associated with ribosomes in dendrites (Job and Eberwine, 2001). These findings led us to examine the simultaneous translational activities of multiple GluR mRNAs in dendrites. Cellular physiology requires the coordinated regulation of multiple mRNAs and proteins; thus, it is reasonable to presume that the

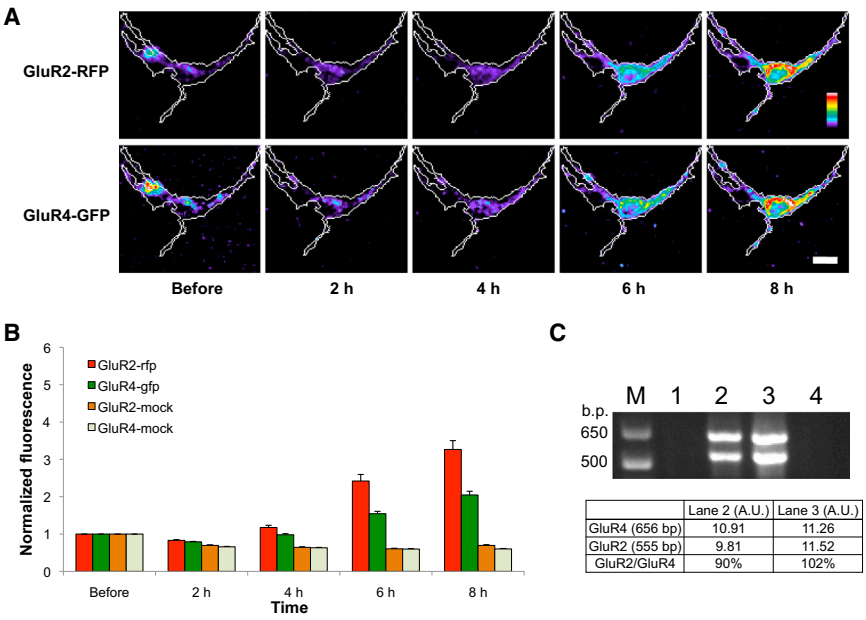

	Lane 2 (A.U.)	Lane 3 (A.U.)
GluR4 (656 bp)	10.91	11.26
GluR2 (555 bp)	9.81	11.52
GluR2/GluR4	90%	102%

Figure 1. GluR2-RFP mRNA Shows Faster Translational Progression than GluR4-GFP mRNA in Hippocampal Neurons

(A) Example fluorescence images of neurons cotransfected with GluR2-RFP and GluR4-GFP mRNAs. Scale bar represents 10 μm.

(B) Bar graphs display the time-dependent increase of the fluorescent intensities of each mRNA and controls from three independent experiments (117 cells for GluR2-RFP and GluR4-GFP mRNAs, and 94 cells for mock transfections). Error bars are SEM.

(C) RT-PCR of a single neuron that was transfected with GluR2-RFP and GluR4-GFP mRNAs shows that comparable amounts of both mRNAs were transfected. Upper panel: M, DNA ladder; lane 1, single neuron without transfection; lane 2, single neuron transfected with GluR2-RFP mRNA and GluR4-GFP mRNA; lane 3, cDNA directly reverse transcribed from GluR2-RFP mRNA and GluR4-GFP mRNA; lane 4, no template. Lower panel: Quantitation of GluR2-RFP and GluR4-GFP PCR products was measured using UltraQuant v6.0 software (Specialty Laboratory). Primers are designed to span GluR ORFs (forward primers) and tomato/wasabi ORFs (reverse primers) and cDNAs are generated using reverse primers on the RNA from a single transfected cell. The control PCRs in lane 3 are generated with equal amounts of starting GluR2-RFP mRNA and GluR4-GFP mRNA in a mixture using the same procedures employed for the single-cell cDNA synthesis.

translation of multiple mRNAs would also be coordinately regulated in order to facilitate biological processes such as learning and memory. However, it remains unclear whether the translational regulation of distinct mRNAs is synchronized.

To examine the dynamics of translational regulation of multiple mRNAs in an individual dendrite, we used in vitro transcription to generate GluR2-tomato red fluorescent protein (RFP)-tagged (hereafter termed GluR2-RFP) mRNA and GluR4-wasabi GFP-tagged (hereafter termed GluR4-GFP) mRNA that retained the original 5′ and 3′ UTRs of mRNA. These reporter mRNAs were then cotransfected at equal amounts into primary rat hippocampal neurons. We monitored translational activities as reflected by the fluorescent signals from the newly synthesized proteins in live neurons in real time. The transfection of in vitro transcribed mRNAs enabled us to observe translational activity without the confounds of transcriptional and RNA trafficking issues associated with DNA transfection. Although there are thousands of mRNAs in dendrites (Buckley et al., 2011; Cajigas et al., 2012; Crino and Eberwine, 1996; Phillips and Eberwine, 1996), we specifically chose to use GluR2- and GluR4-based mRNA constructs for several reasons: (1) AMPARs play important roles in dendritic function; (2) a typical AMPAR consists of a tetramer of proteins comprised of two GluR2 subunits and two dimers of either GluR1, GluR3, or GluR4, showing that the demands for GluR2 and GluR4 are not equivalent; and (3) these two mRNAs have similar abundances and half-lives (8.19 hr for GluR2 and 8.27 hr for GluR4), which enabled us to more readily assess translational regulation (Mameli et al., 2007; Miyashiro et al., 1994; Sharova et al., 2009; Sutton et al., 2004). Here, we show that two different dendritically localized mRNAs can exhibit distinctive time- and location-dependent translational bursts, suggesting that functionally isolated subregions within a dendrite have the ability to differentially regulate distinct mRNAs (Kacharmina et al., 2000).

RESULTS

GluR2-RFP mRNA Is Translated More Rapidly than GluR4-GFP mRNA in the Soma

Equal amounts of GluR2-RFP mRNA and GluR4-GFP mRNA were transfected into rat hippocampal neuronal cultures at 3–14 days in vitro (DIV), followed by real-time monitoring of their translational activities by fluorescence using confocal microscopy (Figure 1). These transfected cells displayed noticeable increases in fluorescence over a 4 hr posttransfection period as compared with mock-transfected cells (Figures 1A and 1B). We tracked 117 dual-transfected and 94 mock-transfected neurons, and observed significant cell-to-cell variation in translational responsiveness. The presence of transfected mRNAs in dendrites was verified by RT-PCR and in situ hybridization using probes specific to the transfected RNAs, which also showed that comparable amounts of both mRNAs were transfected (Figure 1C) and that the transfected mRNAs were not differentially degraded (Figure S1). The increase in signal from the GluR2-RFP mRNA occurred more rapidly and reached a higher level in the cell body over a longer time window (up to 8 hr with a 2 hr interval) compared with that from the GluR4-GFP mRNA, which led us to ask whether dendritic local translation is similar to somatic translation.

The Local Translational Hotspots of GluR2-RFP and GluR4-GFP mRNAs Show Both Overlapping and Distinct Distribution Patterns

After we examined the overall translational activity of the transfected mRNAs over a 2 hr interval, we examined the protein synthesis in dendrites at 5 min intervals to capture the dynamics of newly synthesized proteins. A previous study reported an estimated $t_{1/2}$ for fluorescent protein translation in neurons of

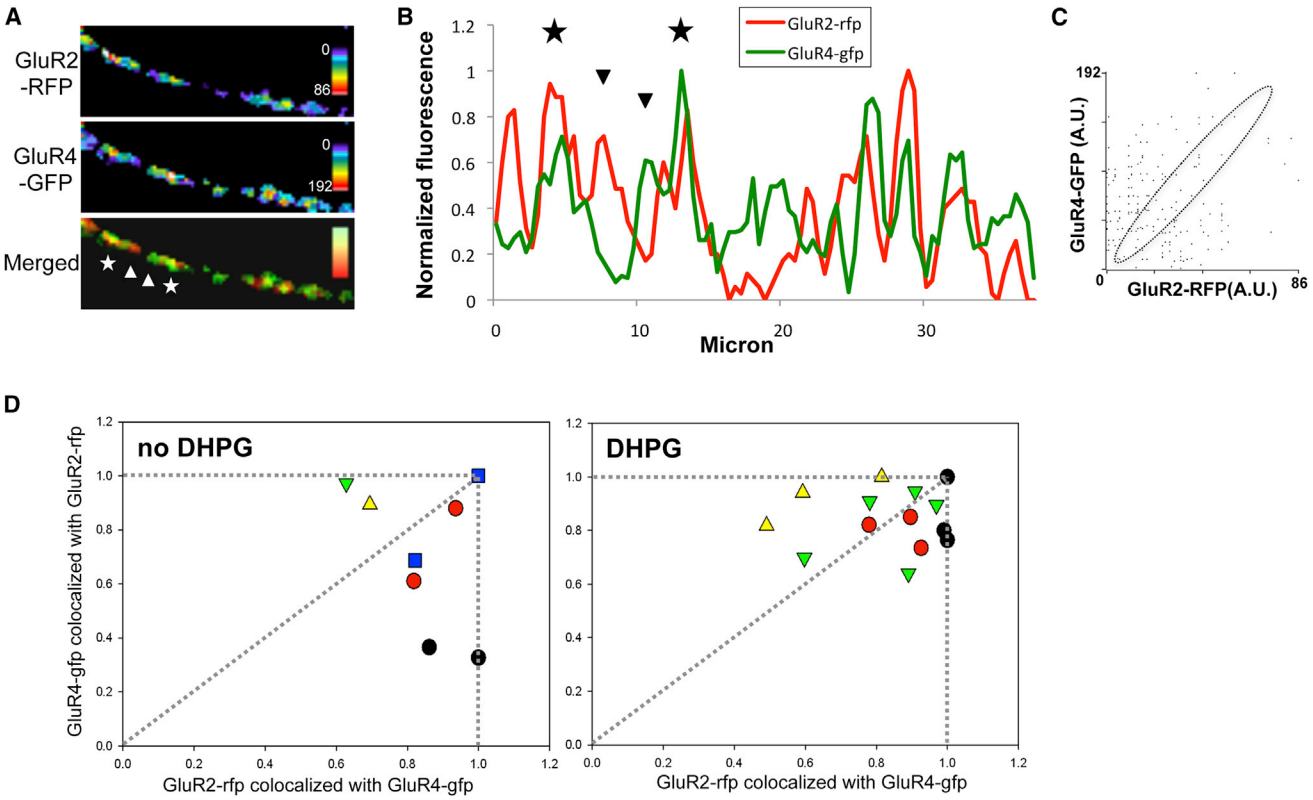

Figure 2. The Translational Hotspots of Two mRNAs Show Distinct Distribution Patterns by Dendrites, and DHPG Treatment Changes Colocalization Features

(A) Fluorescent images of GluR2-RFP and GluR4-GFP without DHPG treatment. Examples of colocalized hotspots (stars) and offset area (arrowheads) are displayed.

(B) Line graphs of normalized fluorescence from fluorescent images (Figure 2A) display the feature of colocalization of hotspots without DHPG treatment.

(C) Scatterplot showing colocalized pixels (within dotted oval) between GluR2-RFP and GluR4-GFP.

(D) Colocalized translation features are displayed on a scatterplot (see text for details). The same symbols represent the dendrites from the same cell for each treatment condition. Colocalization coordinates are calculated at 10 min after DHPG treatment and at the same time point for no DHPG treatment.

approximately 7 min and showed that rapid translation was completed within 15 min (Job and Eberwine, 2001). Translational hotspots of GluR2-RFP and GluR4-GFP are seen as puncta along the dendrite at any given time (Figure 2A). In order to examine the colocalization of GluR2-RFP and GluR4-GFP in particular hotspots, we created a one-dimensional, three-pixel-wide mask over each dendrite and used image processing software (Metamorph) to measure red and green fluorescent signals along the spatial transect. For each signal, we normalized the fluorescence values based on the maximum fluorescent signal over all times and locations. We assessed the colocalized signal of the two proteins by defining areas where both signals were greater than the threshold of 15% of the normalized fluorescence, which removed the noise and background. These data highlighted the fact that although some GluR2-RFP and GluR4-GFP peaks showed overlap (Figures 2A and 2B, stars), the two protein peaks were offset from each other at other locations (Figures 2A and 2B, arrowheads). The scatterplot depicting the colocalization coefficients of GluR2-RFP and GluR4-GFP also shows that many pixels are not colocalized (Figure 2C). In addition to the spatial differences, the levels of the normalized signal of the two proteins at the same hotspot also varied by location, reflecting different magnitudes of the translational activities of the two mRNAs. We developed a two-dimensional coordinate system to show the proportion of colocalized translation within each dendrite, which illustrated the static colocalized translational features of multiple dendrites on a single graph (Figure 2D, right panel: dendrites treated with *s*-3,5-dihydroxy-phenylglycine [DHPG], left panel: untreated dendrites; also see Table 1). For each dendrite, we computed the proportion of GluR4-GFP-expressing pixels in which GluR2-RFP was also coexpressed and plotted the value on the x axis (Figure 2D, left and right panels). We also computed the proportion of GluR2-RFP-expressing pixels that also coexpressed with GluR4-GFP and plotted this value on the y axis (Figure 2D, left and right panels; see Experimental Procedures). The figure illustrates the unique colocalization features of each dendrite at the moment of data capture (Figure 2D, left panel). To determine whether the degree of colocalized translation was altered when local protein synthesis was stimulated, we used DHPG to stimulate dendritic translation (Job and Eberwine, 2001; Ju et al., 2004; Kacharmina et al., 2000; Weiler and Greenough, 1993). We examined five cells

Table 1. Contingency Table for the Colocalization Feature of GluR2-RFP and GluR4-GFP

	GluR2-RFP = 1	GluR2-RFP = 0
GluR4-GFP = 1	A	B
GluR4-GFP = 0	C	D

without DHPG treatment and four cells with DHPG treatment, comprising eight and 14 dendrites, respectively. Each dendrite expressed a distinct colocalized translation feature. Dendrites from the same cell or other cells expressed unique colocalization features. DHPG treatment stimulated local translation, leading to an increase of colocalized translation, i.e., the coordinates tended to cluster toward the upper-right area of the plot (Figure 2D, right panel). The results suggest that DHPG increased overall dendritic protein synthesis activities by simultaneously yet distinctly escalating the translation rates of multiple mRNAs. This trend is pronounced for GluR4-GFP ($p = 0.066$, equal variance test), suggesting that some hotspots transition from the preferential translation of GluR2-RFP mRNA to a more general translation of other mRNAs, as indicated by the increased GluR4-GFP translation with DHPG treatment. These results also show that different dendrites, even when attached to the same cell, have unique colocalization features. A multivariance ANOVA (MANOVA) conducted on GluR2-RFP and GluR4-GFP cotranslation patterns (see Experimental Procedures) showed significant differences among different cells. Post hoc tests showed a significant difference in GluR2-RFP translation patterns ($p = 0.034$ for both conditions and $p = 0.005$ only for DHPG), whereas a less significant difference was found for GluR4-RFP translation patterns ($p = 0.174$) among cells. A comparison of the variation between dendrites attached to same cell and the variation across dendrites of different cells revealed that intracellular dendritic variation was as great as intercellular dendritic variation in many cases.

The Dynamics of Cotranslation of Two mRNAs Indicates that Local Translational Regulation Discriminates between GluR2-RFP mRNA and GluR4-GFP mRNA

The observation that the distribution patterns of translational hotspots of GluR2-RFP and GluR4-GFP were variable raised the question: how do translational hotspots change activity over time? To address this issue, we cotransfected the two GluR-reporter mRNAs and performed confocal time-lapse imaging under unstimulated and DHPG-stimulated conditions (Figure 3). In dendrites, the overall protein levels of GluR2-RFP and GluR4-GFP showed a rapid increase in the first 10 min after DHPG treatment and then increased more slowly over the next 30 min, at which point GluR2 translation leveled out. GluR4 translation showed steady rate of increase for the first 30 min and then a slower increase over a 60 min time period (Figure S2). To show that the translational rates were dictated by the mRNA sequences encoding the *gria* genes rather than the specific reporter proteins, we used a distinct GFP to tag both GluR2 and GluR4 mRNAs. We independently transfected these two mRNAs (GluR2-GFP mRNA and GluR4-GFP mRNA) and examined their local dendritic translational dynamics. In agreement with the GluR2-tomato mRNA and GluR4-wasabi mRNA cotransfection studies, the results show that GluR4-GFP mRNA displays elevated translational activities in comparison with GluR2-GFP mRNA (Figures S2 and S3). However, the individual hotspots of GluR2-RFP and GluR4-GFP showed variable dynamics in terms of peak amplitude and peak width (Figures 3A and 3B). For example, as shown in box 1 of Figure 3, GluR2-RFP displayed prominent double peaks of expression after 15 min, whereas GluR4-GFP displayed double peaks prior to DHPG treatment that lasted until 55 min, revealing different translational dynamics for the two mRNAs. Box 2 in Figure 3B shows a representative spatial region in which GluR2-RFP displayed oscillating levels of translation, but GluR4-GFP hotspots retained high levels of translation. These results show that different translational hotspots exhibit differential translational regulation for specific mRNAs and that translational hotspots are not homogeneous. This further demonstrates that two different hotspots (i.e., hotspots for GluR2-RFP and hotspots for GluR4-GFP) can exist independently and exhibit independent translational dynamics.

The translational profiles displaying the time-lapse data of normalized fluorescence along the dendrite (Figures 3A and 3B) allowed us to compare individual hotspots within a single dendrite. However, we also wanted to assess the global consequences of having multiple hotspots in multiple dendrites. To accomplish this, we displayed time-lapse colocalized translation coordinates (defined for Figure 2) of each dendrite on a plot to show that the colocalized translation of two proteins continually changed over time (Figures 3C and S4). The degree of colocalized translation changed differently over time between cells and between dendrites of the same cell. There was no consistently reoccurring pattern, with one exception: the trajectories of colocalized translation remained compact in some dendrites but were dispersed in other dendrites, suggesting that the dynamic range of responsiveness between hotspots varied from one dendrite to another. We repeated the time-lapse imaging of transfected cells without DHPG treatment to compare the effects of DHPG on local translation. The dynamic variability in colocalized expression pattern (as measured by the average squared dispersion of the points around the centroid for the coordinates shown in Figures 3C and S4) was 0.220 for DHPG (11 dendrites) and 0.434 for no-DHPG (seven dendrites). The difference between the two sets of dispersion dynamics was significant by an F test (ratio of squared dispersions, $p < 0.0002$, df = 143 and 91; Figure 3D). This result is consistent with the result from Figure 2D, which shows that DHPG stimulation increases the overall translation of multiple mRNAs, potentially resulting in the saturation of the translational capacity of hotspots. These data suggest that once a hotspot is stimulated, it may be desensitized to subsequent stimuli and have limited responses to subsequent plasticity events.

Individual Translational Hotspots Display their Own Characteristics

Since previous studies have shown a positive correlation between the rate of translation and the local concentration of ribosomes, suggesting the existence of subregions within dendrites that are specialized in translation, we next determined whether specific translational attributes are hard-wired to specific locations in the dendrite (Aakalu et al., 2001; Job and Eberwine,

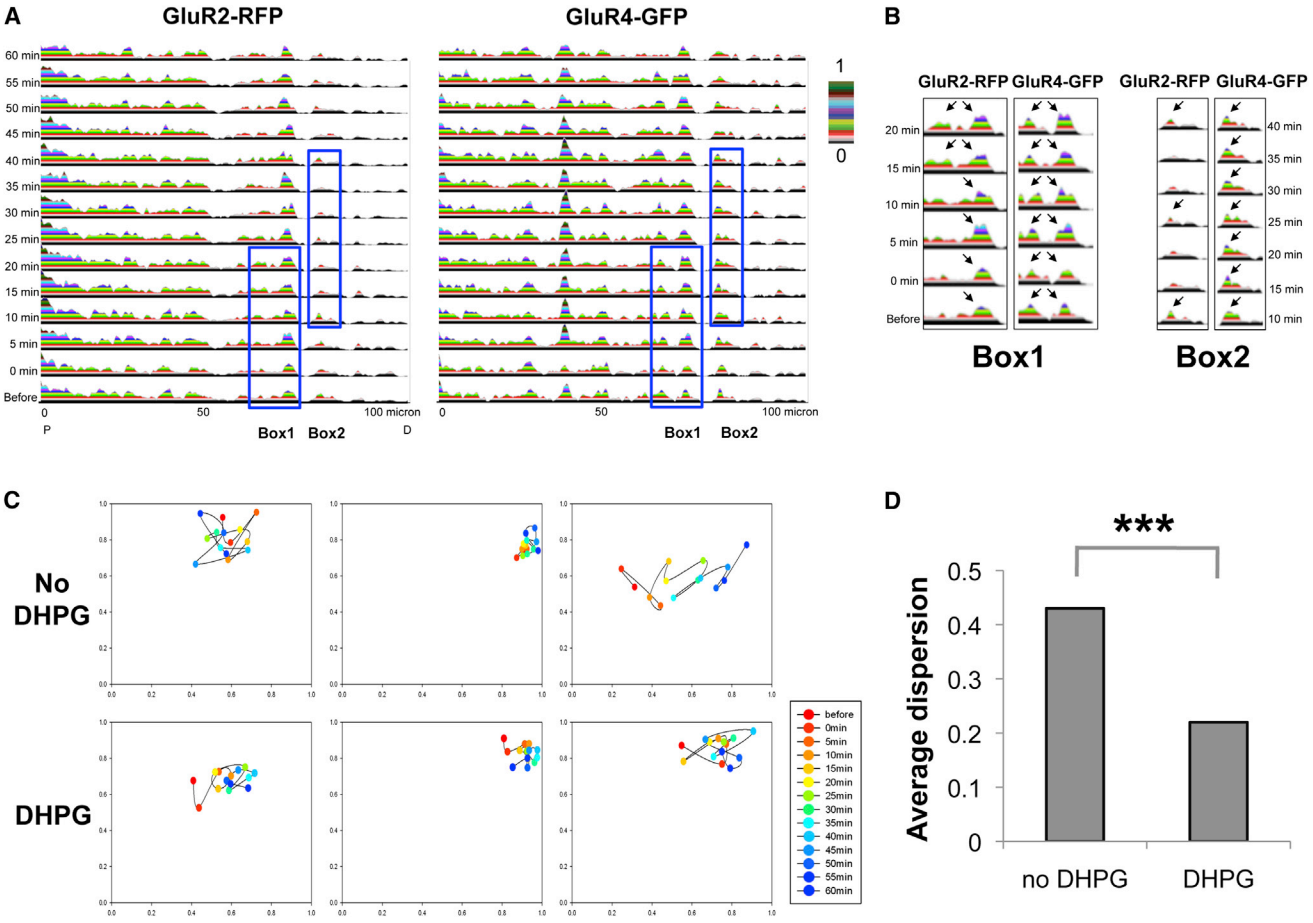

Figure 3. The Protein-Synthesis Activities of GluR2-RFP and GluR4-GFP Are Dynamic

(A) Normalized fluorescence profiles display temporally dynamic changes of protein synthesis. D, distal end of dendrite; P, proximal end of dendrite.

(B) Magnified boxes 1 and 2.

(C) Scatterplot showing time-dependent changes in the colocalization features of non-DHPG-treated and DHPG-treated dendrites.

(D) Average dispersion of the points around the centroid for the coordinates. ***$p < 0.001$.

2001). We calculated the correlation coefficient between the two GluR-reporter protein intensities over time at each location along the length of the dendrite. The blue bars in Figures 4A, S5, and S6 show the magnitude of temporal correlation for each pixel for those locations that were significantly correlated ($p < 0.05$). The overlaid thick red and green lines in Figures 4A, S5, and S6 show the estimated translational hotspots for GluR2-RFP and GluR4-GFP, respectively (see Experimental Procedures). Figure 4A shows that the estimated hotspots of GluR2-RFP and GluR4-GFP share many spatial domains, but also show differences in their location. Further, the degree of temporal cotranslation of the two proteins differs in distinct locations and is negatively correlated in some locations. The subregions of significant negative correlation are hypothesized to represent dendritic domains with different coregulatory mechanisms for translation of the two proteins.

We examined 20 dendrites from nine cells (13 DHPG-treated dendrites from four cells and seven non-DHPG-treated dendrites from five cells). A comparison of DHPG-treated dendrites and non-DHPG-treated dendrites showed that the average temporal correlation coefficient of GluR2 and GluR4 expression in DHPG-treated dendrites (correlation = 0.344) was significantly lower than that in nontreated dendrites (correlation = 0.408, $p < 0.001$; Figure 4B), suggesting that DHPG increases the specific translation of one protein or saturates the temporal response variation. However, the percentage of negatively correlated hotspots was similar between DHPG-treated and nontreated dendrites (DHPG = 13.1% and non-DHPG 14.7%, $p = 0.608$; Figure 4C), suggesting that these negatively correlated domains do not participate in the DHPG response. The mean width of locations in which GluR2 and GluR4 were highly correlated was also similar between treated and nontreated dendrites (4.96 pixels for DHPG and 5.38 pixels for non-DHPG), suggesting that the size of translation-specialized subregions is not affected by DHPG (Figure 4D).

To show the specificity of the translational response, we generated a randomized data set through permutation of the original values. We then analyzed this data set as we had done

for the original data sets (Figure S7). The artificially generated data set showed no temporal correlation of cotranslation for the two proteins. The correlation coefficient was 0.264 for the original data, compared with 0.037 for permutated data. This shows that dendrites contain subregions that are specialized in translation, and the cotranslation of the two mRNAs is not stochastic.

In order to summarize the spatial characteristics of the dynamic translation response, we grouped the time-lapse data into three phases (early [mean intensity of t_{5min}–t_{20min}], middle [mean of t_{25min}–t_{40min}], and late phase [mean of t_{45min}–t_{60min}]) and then tabulated the translational dynamics as discrete categories (Figure 4E). We categorized the translational dynamics of each phase according to its responsiveness and illustrated it in four colors: continuous increase (red), peak at middle phase (yellow), valley at middle phase (blue), or continuous decline (green). In Figure 4E, we display the ratios between these categories of responsiveness, as highlighted by their colors aligned over the length of the dendrite from proximal to distal ends. These data show that the proportions of the response categories are highly variable along the spatial dimensions of the dendrites without a clear proximal-to-distal pattern, suggesting a location-specific governance of translational regulation rather than a simple spatial distance from the soma. A prominent aspect of Figure 4E is that the nontreated dendrites display a larger proportion of continuous increases (red) than the DHPG-treated dendrites (Figure 4F). This again shows that most regions of dendrites show continuous increases in protein levels, but upon stimulation with DHPG they switch to more complex temporal dynamics that are dependent on the spatial location along the dendrites.

Photoconversion of GluR2-Kaede Protein Highlights Additional Translational Dynamics at Fluorescent Hotspots

The diffusion kinetics and translational inhibitor studies show that the hotspots assessed in this study correspond to localized translation. To further assess this, we made a GluR2-Kaede construct that contained an irreversibly photoconvertible, fluorescent Kaede protein motif at the 3′ end of GluR2 open reading frame (ORF), and then transfected hippocampal neurons with this mRNA. We assessed the characteristics of the original GluR2-Kaede protein producing green fluorescence (green GluR2-Kaede), the photoconverted proteins in which the green GluR2-Kaede was irreversibly converted to red fluorescent GluR2-Kaede (red GluR2-Kaede), and the newly generated green GluR2-Kaede protein within the photoconverted red GluR2-Kaede hotspot. Illumination by a 405 nm laser at the hotspots instantly photoconverted green GluR2-Kaede proteins into red GluR2-Kaede proteins (Figures 5A and 5B). The photoconversion increased the red fluorescent signal of the hotspots by 2.5-fold (mean = 2.49-fold, SEM = 0.21, n = 10) and reduced the green fluorescent signal of the hotspots below 20% (mean = 0.18-fold, n = 10). Following photoconversion, we asked whether the red GluR2-Kaede diffused away by measuring the decrease in red fluorescence of the GluR2-Kaede hotspots. To this end, we drew a line across a red hotspot and set two flanking boundaries on each side of the maximal red fluorescence in the hotspot where red fluorescent values were half of the maximum value (Figure 5B). We then evaluated the diffusion of red GluR2-Kaede protein by measuring the change in the distance between the flanking boundaries (Figure 5C), as this distance would greatly increase if diffusion were occurring. The results show that the majority of photoconverted red GluR2-Kaede molecules did not move (±6% width change), and retained their spatially resolved location for longer than the 5 min window of observation. Although the majority of red GluR2-Kaede proteins did not move, the mean fluorescence of the red GluR2-Kaede area slowly decreased to 90% of the initial mean fluorescence after 5 min, suggesting either photobleaching of the signal or a reduction in protein abundance (Figure 5D). To complement these measurements, we also monitored the increase of green GluR2-Kaede proteins in the photoconverted hotspots (Figure 5D). The green GluR2-Kaede continued to increase to 120% of the original value 5 min after photoconversion. We repeated the GluR2-Kaede photoconversion experiments with DHPG treatment to assess stimulated protein synthesis, as well as with translational inhibitors to show that the increase in newly observed green GluR2-Kaede fluorescence is protein synthesis dependent (Figure 5E). As shown for our earlier constructs (GluR2-RFP and GluR4-GFP mRNAs), DHPG treatment increased the translation rate of newly observed green GluR2-Kaede proteins, whereas translation inhibitors inhibited the translation of green GluR2-Kaede at the photoconverted red GluR2-Kaede fluorescent hotspots. These data show no detectable GluR2-Kaede protein diffusion within this time interval, which is consistent with the hypothesis that the new green GluR2-Kaede protein results from local protein synthesis.

DISCUSSION

The cotransfection of two differentially labeled GluR mRNA species allowed us to examine the simultaneous translation of multiple dendritic mRNAs in response to pharmacologic stimulation in a quantitative and precise manner. Previous studies employed fluorescent protein mRNA as an instant readout of translation in live cells and demonstrated that several minutes were sufficient to detect fluorescent signal changes from newly synthesized proteins (Eberwine et al., 2001; Job and Eberwine, 2001). Other studies also detected a significant increase of newly synthesized proteins in dendrites by 10–15 min after stimulation (Dieterich et al., 2010; Gong et al., 2006). In this study, we found that local dendritic translational activity occurred rapidly enough for us to observe the effects of translational stimulation (DHPG) and inhibition (anisomycin) within 5–10 min of treatment (Figure S2), demonstrating that 5 min time intervals were adequate for capturing translational dynamics.

It is reasonable to hypothesize that translational regulation of selected mRNAs is linked to the function of specific subcellular sites, such as an acute demand for the activity of a specific subtype of receptors in a dendritic spine (Branco et al., 2010; Huber et al., 2000; Kwon and Sabatini, 2011; Mameli et al., 2007; Schmid et al., 2008; Sutton et al., 2004). Given this scenario, a cell may utilize different translational rates of distinct mRNAs to produce adequate amounts and ratios of the required proteins. Our results showed that dendrites, even from the same cell,

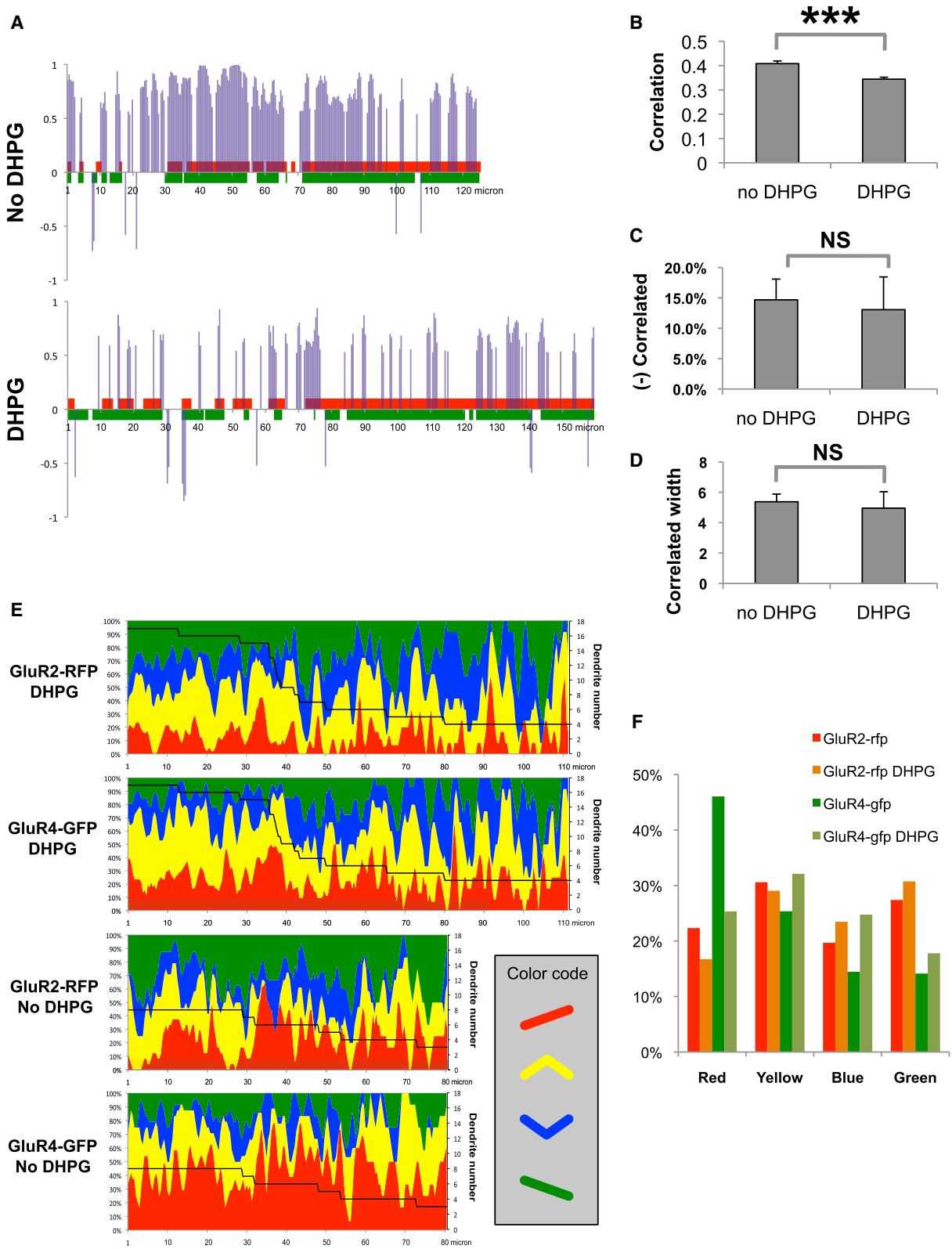

Figure 4. The Characteristics of Translational Hotspots Are Heterogeneous along and among Dendrites

(A) Blue bar graphs show significant temporal correlation coefficient values ($p < 0.05$) at each location along with the estimated translational hotspots of GluR2-RFP (red) and GluR4-GFP (green) shown as thick horizontal bars.

(legend continued on next page)

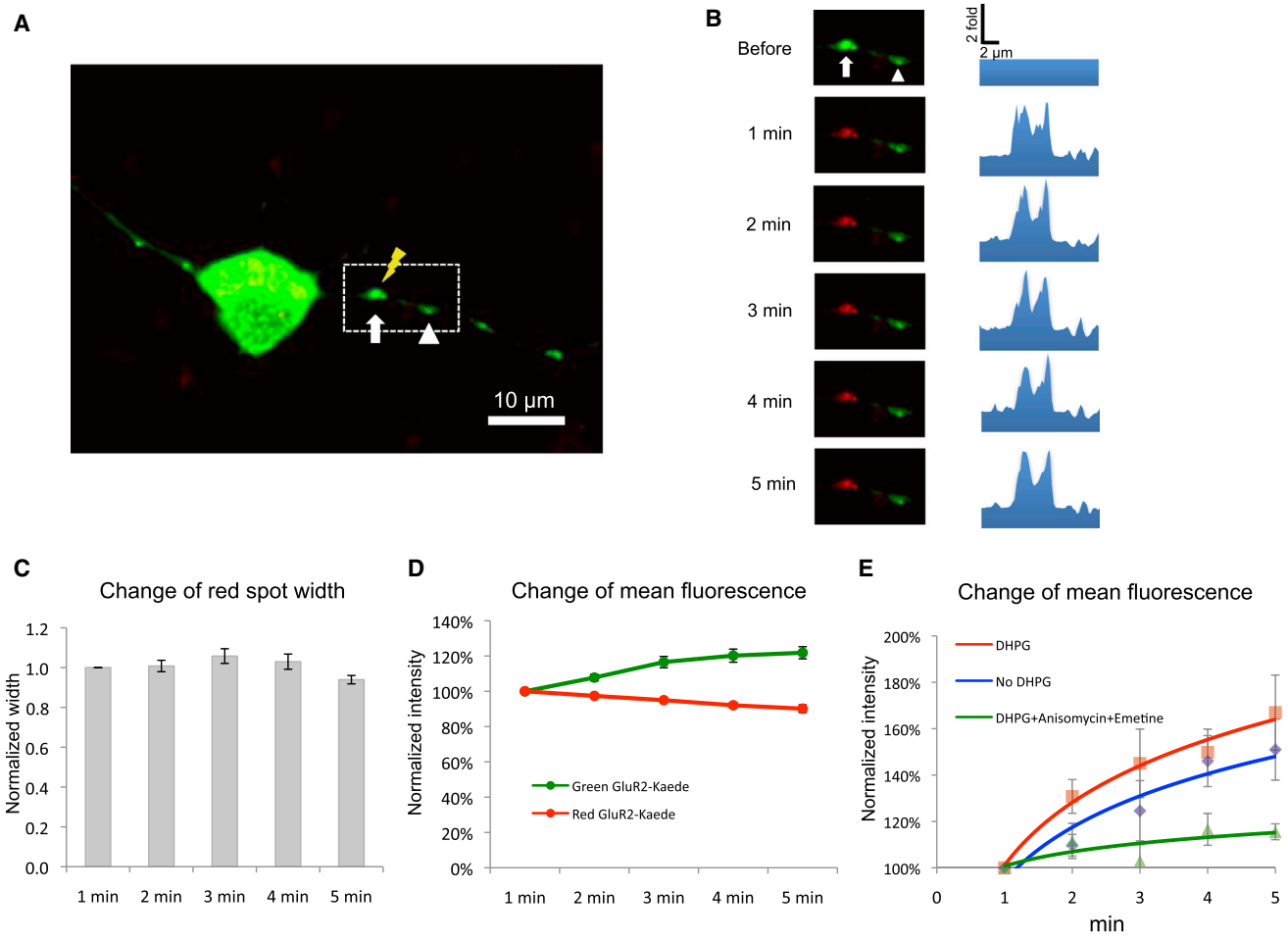

Figure 5. Photoconversion of GluR2-Kaede Protein Shows Limited Protein Movement within Hotspots, and Degradation and Synthesis of Proteins at the Hotspots

(A) A fluorescence image shows translational hotspots indicated by green GluR2-Kaede. An arrow indicates a hotspot illuminated with a 405 nm laser (lightning symbol) and an arrowhead indicates a hotspot without 405 nm laser illumination.

(B) Left: magnified time-lapse fluorescence images from (A). Right: changes in normalized red fluorescent values over a photoconverted hotspot (arrow).

(C) Change in the width of the red fluorescent area over time after photoconversion (n = 10, error bar is ±SEM).

(D) Change in the mean fluorescent value of red and green fluorescence after photoconversion.

(E) DHPG and translational inhibitors change the new green GluR2-Kaede protein-synthesis rates at the hotspots. DHPG-treated hotspots show increased translational activity (red, n = 7) compared with non-DHPG-treated hotspots (blue, n = 4), whereas addition of translation inhibitors (green, n = 5, anisomycin 50 μM and emetine 5 μM) to DHPG-treated hotspots shows attenuated translation at the hotspots. Error bars are SEM.

have different colocalized translation features (static dissimilarity; Figure 2D) and the degree of colocalized translation changes with time (Figure 3C). This suggests a specific dynamic modulation of differential translational regulation in micron-scale subdendritic locations.

DHPG treatment showed how the local translational regulatory system reacted to extracellular stimulation. The translation of GluR2-RFP and GluR4-GFP mRNAs showed broad temporal correlations at subregions along the dendrites. The averaged absolute temporal correlation of dendrites for the two proteins is 0.444 for DHPG-treated dendrites and 0.510 for non-DHP-treated dendrites, which is a small but highly significant difference. When we used a significant correlation value cutoff of 0.85 (which is a $p < 0.05$ for Bonferroni correction of 200 pixels),

(B) The overall temporal correlation of DHPG-treated dendrites shows a lower correlation coefficient than that of non-DHPG-treated dendrites.

(C) The percentage of negatively correlated locations is not significantly different between non-DHPG-treated and DHPG-treated dendrites.

(D) The mean width of the correlated area is not significantly different between non-DHPG-treated and DHPG-treated dendrites. ***$p < 0.001$. NS, not significant. Error bars are SEM.

(E) Area graph shows the proportion of different dynamical types of translational hotspots along dendrites (the color codes for the types are shown in the inset). The dendrite numbers used in the calculation are shown as black horizontal lines.

(F) Bar graphs show the percentages of hotspot types (colors) from each panel in Figure 4F.

13.4% of the pixels show a significant correlation at $p < 0.05$ in nontreated dendrites, while only 6.0% of the pixels are significantly correlated in DHPG-treated dendrites. Thus, DHPG treatment seems to cause translational hotspots to lose temporal coherence between the two proteins during the increase in general translation of multiple mRNAs. This may be due to mRNA/protein-specific translational responses. The occurrence of highly correlated spots per unit length was not different between DHPG and non-DHPG treatments (mean of correlated area numbers per unit length = 0.09 in non-DHPG and 0.10 in DHPG; $p = 0.260$). This suggests that subregions of the dendrite may respond to DHPG stimulation in a differentially regulated manner and that the nature of the regulated response is dictated by the spatial location. To assess the potential for diffusion to affect our data, we used a diffusion model (detrending soma gradient) to eliminate the possibility of somatic protein complication, comprehensively investigated the results to test the inclusion of any bias during the experiment or analysis, and examined the continuity of translational hotspots (diffusion from) over the 1 hr time periods (Figure S8 shows very little movement from the point of synthesis over an extended time period). These results preclude somatic influx, diffusion, and the turnover rate of proteins as significant contributors to the results.

One of the major concerns in studying local dendritic translation is the difficulty of linking a marker protein with its translational activity. We used direct transfection of mRNAs into neurons because this method has been shown to be effective (Job and Eberwine, 2001) and rapid enough to detect developing translational hotspots (translational hotspots can be detected as early as 4 hr after the transfection). To confirm that the translational hotspot dynamics we observed reflect bona fide local translational activities, we employed a photoconvertible, protein-tagged GluR2 construct (GluR2-Kaede). The photoconversion experiments proved that the hotspot dynamics is primarily the result of synthesis and degradation of the proteins and is minimally influenced by protein movements (Figure 5). We also examined the colocalization of secretory pathway structures and hotspots to determine whether the hotspots are part of a trafficking system. The results from costaining of hotspots and endoplasmic reticulum (ER)/Golgi structures show that some hotspots are colocalized with secretory pathway structures, but also quite a few hotspots exist without a relationship with secretory pathways (Figure S9). Based on photoconversion and colocalization results, we conclude that translational hotspots in the dendrite genuinely reflect the local translational activities.

Based on the above observations, we propose a model in which most local dendritic translation occurs in specific subregions (i.e., translation-specialized subregions). In these specific subregions, the translational machinery is clustered and the type of regulatory dynamics is determined by the local aggregation of ribonucleoproteins (RNPs) and translational machinery, allowing for structural plasticity within the dendrite. Within each micron-scale region, proteins are synthesized with differential regulation in response to stimuli, but the type of regulatory dynamics is specific to the region (Figure 6A). Based on this model, we hypothesize that DHPG stimulation causes preferential recruitment of selected mRNAs to be translated, or that translational inhibition of mRNAs is diminished, without alterations in the size or number of hotspots. Consequently, the hotspots become more selective in translation of particular mRNAs, giving rise to an overall increase in protein synthesis over the length of the dendrite, while decreasing the temporal correlation of the translation of the two proteins (Figure 6B).

These results have important implications for the role of local dendritic translation in long-term potentiation (LTP). LTP is known to require local protein synthesis; however, it has been unclear whether local translation is regulated through the simultaneous global control of all localized mRNAs or is controlled by mRNA-specific mechanisms. Further, if local translation regulation employs mRNA-specific mechanisms, it is unclear which elements modulate the regulatory process (Kang and Schuman, 1996; Kelleher et al., 2004; Lynch, 2004). Our results show that multiple mRNAs can be translated at any particular translation-specialized subregion, although specific mRNAs can have different translational rates. This gradient of stimulated local translations suggests that distinct hotspots may have different translational thresholds necessary to participate in LTP or LTD in specified regions of the dendrite. Because a particular mRNA can have different translational dynamics (see color codes in Figure 4E) within different hotspots of the same dendrite, it is logical to speculate that LTP/LDP-mediated local translation is governed by the nature of the hotspot, and not solely by the mRNA primary sequence, structure, or quantity (Figure 1C).

EXPERIMENTAL PROCEDURES

GluR and Fluorescence Protein Motif Fusion Plasmids and In Vitro Transcription of mRNA

Fluorescent protein motif-fused mRNAs using GluR2 mRNA (NCBI Reference Sequence: NM_001083811.1), GluR4 mRNA (NCBI Reference Sequence: NM_017263.2), RFP tdTomato gene (GenBank: AY678269.1), and GFP mWasabi gene (GenBank: EU024648.1) were designed in which a fluorescent motif was inserted between the end of the ORF and the beginning of the 3′ UTR. The designed fusion constructs were synthesized using the gene synthesis service from GenScript and cloned into pCDNA3.1(+) plasmid. The constructs were confirmed by sequencing. mRNAs were synthesized in vitro using the mMessage mMachine T7 kit (Ambion) with poly (A) tails according to the manufacturer's recommendation. In vitro transcribed mRNAs were quantified and qualified using a NanoDrop (Thermo Scientific) and 2100 Bioanalyzer (Agilent Technology). We also synthesized GluR2-GFP mRNA and GluR4-GFP mRNA to examine the chromophore effect on translation.

Cell Culture and mRNA Transfection

Primary rat hippocampal neurons were prepared from embryonic rats (E18; Sprague Dawley) and cultured on glass coverslips with neurobasal medium (NB) supplemented with B-27 supplement (5% CO_2, 37°C). Three to 14 days after planting, the neurons were washed with NB and transfected. mRNA transfection was performed using the TransMessenger Transfection Reagent Kit (QIAGEN). Then 1 μg of GluR2-RFP mRNA and 1 μg of GluR4-GFP mRNA were added to the mixture of EnhancerR (4 μl) in buffer ERC (x μl to make a final volume of 100 μl) following incubation for 5 min at room temperature. After the incubation, 8 μl of TransMessenger transfection reagent was added to the mRNA-EnhancerR mixture and incubated for 10 min at room temperature. Then 900 μl of NB was added to the mRNA-lipid mixture and the transfection complex was dropped onto neurons (500 μl per coverslip). As an alternative transfection regime, 1 pM of PepFect 6 reagent (Andaloussi et al., 2011) was added to the mRNA-lipid mixture to increase the transfection

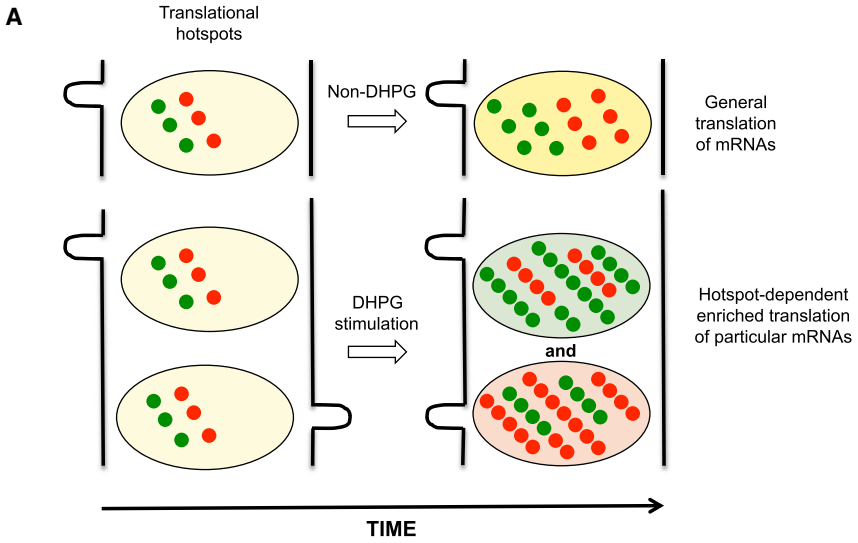

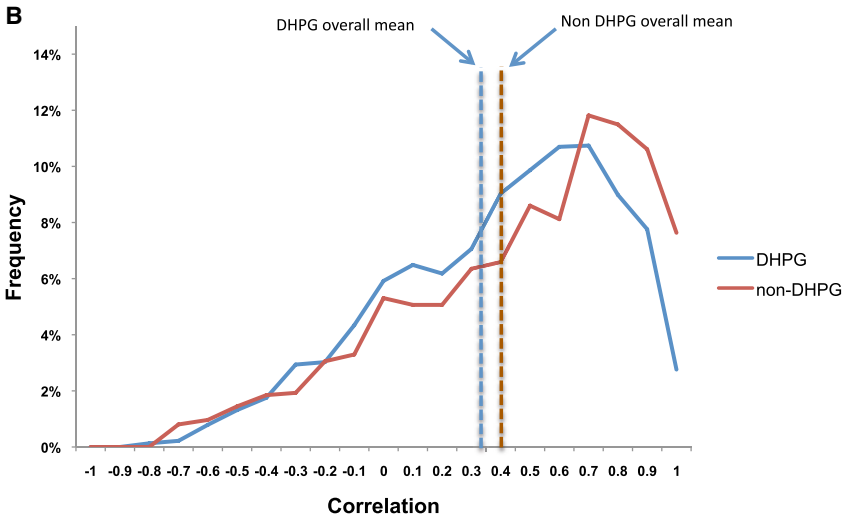

Figure 6. Model for Showing Differently Reacting Translational Hotspots in Non-DHPG-Treated and DHPG-Treated Dendrites

(A) Translational hotspots at which translational machinery is clustered produce GluR2-RFP or GluR4-GFP (red circle: GluR2-RFP; green circle: GluR4-GFP). With DHPG stimulation of local translation, the hotspots rapidly increase protein synthesis with different translational rates of particular mRNAs depending on the hotspot kinetics. Meanwhile, hotspots in non-DHPG-treated dendrites produce proteins moderately.

(B) The distribution of temporal correlation coefficient values between GluR2-RFP and GluR4-GFP translations (blue, DHPG; red, non-DHPG) shows that DHPG-treated dendrites have less temporally correlated locations than nontreated dendrites. The means of the correlation coefficient of overall dendrites (dashed line) are indicated.

efficiency. Neurons with the transfection complex were incubated under normal incubation conditions and the transfection complex containing media was replaced by normal NB/B-27 media after 1 hr. Then, 6–8 hr after initiation of transfection, the neurons were washed with rat saline (140 mM NaCl, 5.4 mM KCl, 1 mM $MgCl_2$, 2 mM $CaCl_2$, 16 mM glucose, 10 mM HEPES, pH 7.3) and transferred to an imaging bath chamber (Warner Instruments) with rat saline for live-cell imaging.

Confocal Microscopy and Data Acquisition

Live neurons in the bath chamber was placed on a heating stage and kept at 37°C throughout the imaging process. Confocal red and green fluorescent images were captured with an LSM 510 or LSM 710 confocal microscope system (Zeiss). To stimulate local translation, 50 μM of DHPG was added (t_0) 5 min after the baseline imaging (t_{Base}). For the translation inhibition experiment, 10 μM of anisomycin or 50 μM of anisomycin plus 5 μM of emetine was added with 50 μM of DHPG (t_0). Captured fluorescent images were processed with background correction and a median filter using MetaMorph Image Analysis Software (Molecular Devices), and fluorescent values were acquired by drawing a line over a dendrite and measuring the mean value from a three-pixel width from the line. The fluorescent values were normalized based on the maximum fluorescent values of each dendrite. To observe overall protein synthesis activity, regions of interest were drawn around the cell body and the mean fluorescent intensity was measured and normalized based on mean values from before-transfection images.

Data Analysis

Colocalization Coordinate Calculation

Each pixel was assigned a value of one (above the threshold, 15%) or zero (below the threshold), and then each pixel was enumerated as one of four possible combinations of GluR2-RFP = 0 or 1 and GluR4-GFP = 0 or 1, resulting in a contingency table (Table 1). Then the percentage of GluR2-RFP pixels that coincidently localized with GluR4-GFP pixels above the threshold among the total GluR2-RFP pixels above the threshold was calculated (x), A/(A+C) in Table 1. Conversely, the percentage of GluR4-GFP pixels that coincidently localized with GluR2-RFP pixels above the threshold was calculated (y), A/(A+B) in Table 1.

MANOVA of the Colocalization Pattern

The colocalized translation coordinates were bias corrected by Laplace transform and then logit transformed to yield approximately normal values. The variance of GluR2-RFP and GluR4-GFP colocalized translation patterns was tested using a MANOVA, with logit transform of GluR2-RFP and GluR4-GFP as the response variables, DHPG as fixed effects, and cell identity as nested within DHPG. Both GluR2-RFP and GluR4-GFP were subsequently tested separately in a general linear model ANOVA.

Noise Reduction

Fluorescence measurements are subject to noise along space (i.e., proximal-to-distal locations along the dendrite) and time. To remove noise, we applied a discrete Gaussian smoothing kernel in both the spatial dimension (window size 5 at ±1 and ±1.5 SD) and the time dimension (window size 3 at ±1.5 SD).

Detrending the Soma Gradient

To identify regions of high translational activity ("the estimated translational hotspots"), we first computed the total protein levels at each spatial location by summing the measurements over time for each pixel unit. We assumed that the measured levels of protein were a composite of a protein diffusion gradient from the soma and local translation within the dendrites. To model soma protein diffusion, we created a model as follows: Let $\rho(x,t)$ be the protein level at position x and time t. We assume that the protein diffuses with a

diffusion coefficient $k1$ from a point source at coordinate $x = 0$ (soma) with a no-flux boundary (i.e., cannot diffuse out) at $x = 1$ (normalized end of a dendrite). That is, we assume a boundary condition of $d\rho/dx = 0, x = 1$. We also assume that the protein is degraded or the signal is lost with a first-order kinetics rate $k2$ uniformly at all locations. We next assume that there is a constant flux of protein supply at rate $k3$ at $x = 0$ (soma). That is, we assume another boundary condition of $k2 \bullet (d\rho/dx) = -k3$. The diffusion equation is given by $\partial\rho/\partial t = k1(\partial^2\rho/\partial x^2) - k2 \bullet \rho$ Assuming that the measurements are done at steady state of the soma diffusion process, we solve for steady-state solutions, yielding

$$\rho(x) = C \bullet \frac{^{-b(x-2)} + e^{bx}}{1 + e^{2b}} \qquad \text{(Equation 1)}$$

where C is a normalization constant that depends on the flux rate $k3$ at the soma and $b = \sqrt{k2/k1}$. Equation 1 specifies a decreasing gradient from $x = 0$ due to the modeled diffusion from the soma. To identify translational hotspots where protein levels depend on local processes, we estimated the soma diffusion component of protein levels by fitting a gradient model of Equation 1 to the data using a nonlinear regression fit (nls function in R) and subtracting the estimated gradient from each spatial location (detrending the data). We assessed whether the resulting residuals showed any additional soma-to-distal-dendrite trend by fitting a median linear regression to the residuals and assessing the slope of the regression. The median regression procedure was chosen because the residuals represent the local translation output, which is not expected to follow standard regression assumptions. The magnitude of the slope was compared with the 95th percentile range (Q95) of the data. If the slope was less than 25% of Q95, we accepted the values as sufficiently corrected. For data sets that show additional trends, there are two possibilities. First, the spatial series may be too short to allow assessment of a spatial gradient; such measurements were excluded from further analysis. Second, the values in the original data may be too high at the proximal end as a result of including too much of the soma. For those data sets, we truncated the measurements at the proximal end and carried out the detrending correction until our criterion was satisfied.

Correlating the Time Signals of Each Spatial Pixel

For each dendrite, we assessed the temporal dynamic coherence of each spatial location between GluR2-RFP and GluR4-GFP levels by computing a standard Pearson correlation coefficient between the two receptors levels across the measured time points. The significance of the correlation magnitude was computed using the standard normal approximation.

Bonferroni Correction

Statistical values for each pixel are expected to be nonindependent due to spatial dispersion of both the molecules and imaging. Therefore, for significance of overall trends, we applied a conservative Bonferroni correction, which assumes possible complete nonindependence.

In Situ Hybridization and RT-PCR

In situ hybridization was performed as described previously (Buckley et al., 2011). In brief, 4 hr after transfection, cells were fixed in 4% paraformaldehyde (PFA) and permeabilized in 0.2% Triton X-100. The prepared cells were hybridized overnight at 40–45°C with a digoxygenin-labeled tomato and wasabi probes mixture (DIG-probes mixture). The DIG-probes mixture was then labeled using fluorescence conjugated anti-DIG antibodies. Cells were observed with an LSM 710 microscope system. For RT-PCR, the dendrites and soma were mechanically separated and harvested after 6 hr of transfection using a glass micropipette controlled by micromanipulator. First-strand cDNA was synthesized using reverse transcriptase and then the cDNAs were amplified with primer sets.

GluR2-Kaede Cloning, Photoconversion, and Analyses

The GluR2-Kaede construct was made by cloning Kaede orf (pKaede-S1; MBL International) at the 3′ end of the 5′ UTR-GluR2 ORF. In vitro transcription of GluR2-Kaede mRNA and transfection were carried out as described above. After the transfection, translational hotspots were detected by green fluorescence and a 405 nm laser was illuminated at the hotspots to convert preexisting green GluR2-Kaede to red GluR2-Kaede. Green and red fluorescent signals were captured for 1 min before the photoconversion at 5 s intervals. Time-lapse imaging continued until 5 min after the photoconversion. Fluorescent values were acquired by drawing a line over a hotspot and measuring the mean value from a five-pixel width from the line. Red fluorescent values were normalized based on the mean fluorescent values before the photoconversion of each pixels. Green fluorescent signals were normalized against the mean of 1 min after the photoconversion. The width of the red fluorescent area was determined by finding points on the left and right slopes that had the half value of the maximum value, and then measuring the length between the left and right points. Fluorescent value changes within the hotspot were calculated by measuring the mean red and green fluorescent values within the determined width of the fluorescent areas.

SUPPLEMENTAL INFORMATION

Supplemental Information includes nine figures and can be found with this article online at http://dx.doi.org/10.1016/j.celrep.2013.08.029.

AUTHOR CONTRIBUTIONS

T.K.K. and J.S. carried out experiments. T.K.K., J.S., H.H., U.L., J.K., and J.E. designed experiments and analyzed the data. T.K.K., J.K., and J.E. wrote the manuscript.

ACKNOWLEDGMENTS

We thank Margie Maronski for help with cell culturing, and Dr. Terri Schochet for suggestions and comments on the manuscript. This work was supported in part by a grant from the Swedish Research Council (VR-NT) to U.L., NIMH grant R01-MH888949 to J.K., and an Ellison Foundation Senior Award in Aging and NARSAD Established Investigator grant to J.E. This project was also funded in part by the Penn Genome Frontiers Institute under a grant from the Pennsylvania Department of Health, which disclaims responsibility for any analyses, interpretations, or conclusions.

Received: August 21, 2012
Revised: July 24, 2013
Accepted: August 14, 2013
Published: September 26, 2013

REFERENCES

Aakalu, G., Smith, W.B., Nguyen, N., Jiang, C., and Schuman, E.M. (2001). Dynamic visualization of local protein synthesis in hippocampal neurons. Neuron *30*, 489–502.

Alberini, C.M. (1999). Genes to remember. J. Exp. Biol. *202*, 2887–2891.

Andaloussi, S.E., Lehto, T., Mäger, I., Rosenthal-Aizman, K., Oprea, I.I., Simonson, O.E., Sork, H., Ezzat, K., Copolovici, D.M., Kurrikoff, K., et al. (2011). Design of a peptide-based vector, PepFect6, for efficient delivery of siRNA in cell culture and systemically in vivo. Nucleic Acids Res. *39*, 3972–3987.

Branco, T., Clark, B.A., and Häusser, M. (2010). Dendritic discrimination of temporal input sequences in cortical neurons. Science *329*, 1671–1675.

Buckley, P.T., Lee, M.T., Sul, J.Y., Miyashiro, K.Y., Bell, T.J., Fisher, S.A., Kim, J., and Eberwine, J. (2011). Cytoplasmic intron sequence-retaining transcripts can be dendritically targeted via ID element retrotransposons. Neuron *69*, 877–884.

Cajigas, I.J., Tushev, G., Will, T.J., tom Dieck, S., Fuerst, N., and Schuman, E.M. (2012). The local transcriptome in the synaptic neuropil revealed by deep sequencing and high-resolution imaging. Neuron *74*, 453–466.

Carroll, R.C., Lissin, D.V., von Zastrow, M., Nicoll, R.A., and Malenka, R.C. (1999). Rapid redistribution of glutamate receptors contributes to long-term depression in hippocampal cultures. Nat. Neurosci. *2*, 454–460.

Costa-Mattioli, M., Sossin, W.S., Klann, E., and Sonenberg, N. (2009). Translational control of long-lasting synaptic plasticity and memory. Neuron *61*, 10–26.

Crino, P.B., and Eberwine, J. (1996). Molecular characterization of the dendritic growth cone: regulated mRNA transport and local protein synthesis. Neuron *17*, 1173–1187.

Dieterich, D.C., Hodas, J.J., Gouzer, G., Shadrin, I.Y., Ngo, J.T., Triller, A., Tirrell, D.A., and Schuman, E.M. (2010). In situ visualization and dynamics of newly synthesized proteins in rat hippocampal neurons. Nat. Neurosci. *13*, 897–905.

Dynes, J.L., and Steward, O. (2007). Dynamics of bidirectional transport of Arc mRNA in neuronal dendrites. J. Comp. Neurol. *500*, 433–447.

Eberwine, J., Miyashiro, K., Kacharmina, J.E., and Job, C. (2001). Local translation of classes of mRNAs that are targeted to neuronal dendrites. Proc. Natl. Acad. Sci. USA *98*, 7080–7085.

Eberwine, J., Belt, B., Kacharmina, J.E., and Miyashiro, K. (2002). Analysis of subcellularly localized mRNAs using in situ hybridization, mRNA amplification, and expression profiling. Neurochem. Res. *27*, 1065–1077.

Falley, K., Schütt, J., Iglauer, P., Menke, K., Maas, C., Kneussel, M., Kindler, S., Wouters, F.S., Richter, D., and Kreienkamp, H.J. (2009). Shank1 mRNA: dendritic transport by kinesin and translational control by the 5'untranslated region. Traffic *10*, 844–857.

Goelet, P., Castellucci, V.F., Schacher, S., and Kandel, E.R. (1986). The long and the short of long-term memory—a molecular framework. Nature *322*, 419–422.

Gong, R., Park, C.S., Abbassi, N.R., and Tang, S.J. (2006). Roles of glutamate receptors and the mammalian target of rapamycin (mTOR) signaling pathway in activity-dependent dendritic protein synthesis in hippocampal neurons. J. Biol. Chem. *281*, 18802–18815.

Greger, I.H., and Esteban, J.A. (2007). AMPA receptor biogenesis and trafficking. Curr. Opin. Neurobiol. *17*, 289–297.

Huber, K.M., Kayser, M.S., and Bear, M.F. (2000). Role for rapid dendritic protein synthesis in hippocampal mGluR-dependent long-term depression. Science *288*, 1254–1257.

Job, C., and Eberwine, J. (2001). Identification of sites for exponential translation in living dendrites. Proc. Natl. Acad. Sci. USA *98*, 13037–13042.

Ju, W., Morishita, W., Tsui, J., Gaietta, G., Deerinck, T.J., Adams, S.R., Garner, C.C., Tsien, R.Y., Ellisman, M.H., and Malenka, R.C. (2004). Activity-dependent regulation of dendritic synthesis and trafficking of AMPA receptors. Nat. Neurosci. *7*, 244–253.

Kacharmina, J.E., Job, C., Crino, P., and Eberwine, J. (2000). Stimulation of glutamate receptor protein synthesis and membrane insertion within isolated neuronal dendrites. Proc. Natl. Acad. Sci. USA *97*, 11545–11550.

Kang, H., and Schuman, E.M. (1996). A requirement for local protein synthesis in neurotrophin-induced hippocampal synaptic plasticity. Science *273*, 1402–1406.

Kelleher, R.J., 3rd, Govindarajan, A., and Tonegawa, S. (2004). Translational regulatory mechanisms in persistent forms of synaptic plasticity. Neuron *44*, 59–73.

Kwon, H.B., and Sabatini, B.L. (2011). Glutamate induces de novo growth of functional spines in developing cortex. Nature *474*, 100–104.

Lynch, M.A. (2004). Long-term potentiation and memory. Physiol. Rev. *84*, 87–136.

Mameli, M., Balland, B., Luján, R., and Lüscher, C. (2007). Rapid synthesis and synaptic insertion of GluR2 for mGluR-LTD in the ventral tegmental area. Science *317*, 530–533.

Miyashiro, K., Dichter, M., and Eberwine, J. (1994). On the nature and differential distribution of mRNAs in hippocampal neurites: implications for neuronal functioning. Proc. Natl. Acad. Sci. USA *91*, 10800–10804.

Phillips, J., and Eberwine, J.H. (1996). Antisense RNA amplification: a linear amplification method for analyzing the mRNA population from single living cells. Methods *10*, 283–288.

Riedel, G., Platt, B., and Micheau, J. (2003). Glutamate receptor function in learning and memory. Behav. Brain Res. *140*, 1–47.

Rook, M.S., Lu, M., and Kosik, K.S. (2000). CaMKIIalpha 3′ untranslated region-directed mRNA translocation in living neurons: visualization by GFP linkage. J. Neurosci. *20*, 6385–6393.

Schmid, A., Hallermann, S., Kittel, R.J., Khorramshahi, O., Frölich, A.M., Quentin, C., Rasse, T.M., Mertel, S., Heckmann, M., and Sigrist, S.J. (2008). Activity-dependent site-specific changes of glutamate receptor composition in vivo. Nat. Neurosci. *11*, 659–666.

Sharova, L.V., Sharov, A.A., Nedorezov, T., Piao, Y., Shaik, N., and Ko, M.S. (2009). Database for mRNA half-life of 19 977 genes obtained by DNA microarray analysis of pluripotent and differentiating mouse embryonic stem cells. DNA Res. *16*, 45–58.

Sutton, M.A., and Schuman, E.M. (2005). Local translational control in dendrites and its role in long-term synaptic plasticity. J. Neurobiol. *64*, 116–131.

Sutton, M.A., Wall, N.R., Aakalu, G.N., and Schuman, E.M. (2004). Regulation of dendritic protein synthesis by miniature synaptic events. Science *304*, 1979–1983.

Weiler, I.J., and Greenough, W.T. (1993). Metabotropic glutamate receptors trigger postsynaptic protein synthesis. Proc. Natl. Acad. Sci. USA *90*, 7168–7171.